ISSN 1001-0742
CN 11-2629/X

2012

Volume 24
Number 4

JOURNAL OF ENVIRONMENTAL SCIENCES

ELSEVIER
Science Press

Sponsored by
Research Center for Eco-Environmental Sciences
Chinese Academy of Sciences

ISSN 1001–0742 **Journal of Environmental Sciences** Vol. 24 No. 4 2012

CONTENTS

Serial parameter: CN 11-2629/X*1989*m*210*en*P*27*2012-4

Available online at www.sciencedirect.com
ScienceDirect
Journal of Environmental Sciences 2012, 24(4) 774–780
JOURNAL OF ENVIRONMENTAL SCIENCES
ISSN 1001-0742
CN 11-2629/X
www.jesc.ac.cn

Photocatalytic degradation of perfluorooctanoic acid with β-Ga_2O_3 in anoxic aqueous solution

Baoxiu Zhao[1,2,*], Mou Lv[1], Li Zhou[1]

1. School of Environmental and Municipal Engineering, Qingdao Technological University, Qingdao 266033, China. E-mail: zhaobaoxiu@tsinghua.org.cn
2. State Key Joint Laboratory of Environment Simulation and Pollution Control, Department of Environmental Science and Engineering, Tsinghua University, Beijing 100084, China

Received 05 May 2011; revised 02 August 2011; accepted 16 August 2011

Abstract

Perfluorooctanoic acid (PFOA) is a new-found hazardous persistent organic pollutant, and it is resistant to decomposition by hydroxyl radical (HO·) due to its stable chemical structure and the high electronegativity of fluorine. Photocatalytic reduction of PFOA with β-Ga_2O_3 in anoxic aqueous solution was investigated for the first time, and the results showed that the photoinduced electron (e^-_{cb}) coming from the β-Ga_2O_3 conduction band was the major degradation substance for PFOA, and shorter-chain perfluorinated carboxylic acids (PFCAs, $C_nF_{2n+1}COOH$, $1 \leqslant n \leqslant 6$) were the dominant products. Furthermore, the concentration of F^- was measured by the IC technique and defluorination efficiency was calculated. After 3 hr, the photocatalytic degradation efficiency was 98.8% and defluorination efficiency was 31.6% in the presence of thiosulfate and bubbling N_2. The degradation reaction followed first-order kinetics ($k = 0.0239$ min^{-1}, $t_{1/2} = 0.48$ hr). PFCAs ($C_nF_{2n+1}COOH$, $1 \leqslant n \leqslant 7$) were detected and measured by LC-MS and LC-MS/MS methods. It was deduced that the probable photocatalytic degradation mechanism involves e^-_{cb} attacking the carboxyl of $C_nF_{2n+1}COOH$, resulting in decarboxylation and the generation of C_nF_{2n+1}·. The produced C_nF_{2n+1}· reacted with H_2O, forming $C_nF_{2n+1}OH$, then $C_nF_{2n+1}OH$ underwent HF loss and hydrolysis to form $C_nF_{2n+1}COOH$.

Key words: perfluorooctanoic acid; β-Ga_2O_3; photocatalytic degradation; defluorination; photoinduced electron

DOI: 10.1016/S1001-0742(11)60818-8

Introduction

Perfluorocarboxylic acids (PFCAs, $C_nF_{2n+1}COOH$) have recently caused much concern due to their persistence and bioaccumulative properties (Bischel et al., 2010; Niisoe et al., 2010; Houde et al., 2006; Pistocchi and Loos, 2009). Perfluorooctanoic acid (PFOA, $C_7F_{15}COOH$), as a member of the PFCAs' family, was classified as a likely potential carcinogen by The US EPA's Science Advisory Board in 2006. Recently, PFOA and its precursors have been globally detected in water (Hansen et al., 2002; So et al., 2004), wildlife (Martin et al., 2004; Kannan et al., 2006) and human beings (Tao et al., 2008; Niisoe et al., 2010). So far, no natural decomposition pathway for PFOA has been reported. Hori (2004) and Moriwaki (2005) indicated that it was difficult for most conventional advanced oxidation processes (AOPs) involving hydroxyl radical (HO·) to decompose PFOA. In recent years many efforts have been made to develop effective decomposition or defluorination processes to destroy PFOA, because shorterchain compounds are less bioaccumulative (Kudo et al., 2010; Scott et al., 2006) and cause milder environmental pollution.

At present, treatments for PFOA mainly include photochemical oxidation and sonochemical methods. Hori (2005, 2008) reported that PFOA could be destroyed by photochemical oxidation in the presence of heteropolyacid ($H_3PW_{12}O_{40}$) or persulfate ($S_2O_8^{2-}$), and F and shorter-chain PFCAs were detected as the major products in aqueous solution. Moriwaki (2005) found that PFOA was pyrolyzed at the interfacial region between the cavitation bubbles and the bulk solution in a sonochemical degradation reaction, and F and shorter-chain PFCAs were also identified in the liquid phase. Vecitis (2008) and Cheng (2008, 2010) studied the sonolysis degradation of PFOA and found that the degradation conformed to first-order kinetics and that PFOA was converted to CO, CO_2, F^- and shorter-chain PFCAs. Furthermore, Dillert (2007) reported that PFOA could be decomposed by TiO_2 photocatalytic oxidation, but they found that degradation only occurred in strongly acidic aqueous solution (0.1 mol/L $HClO_4$). Panchangam (2009) also proved that PFOA was only efficiently destroyed by TiO_2 photocatalytic reaction in strongly acidic solution (0.075–0.1 mmol/L $HClO_4$).

To the best of our knowledge, there has been no report on PFOA degradation in anoxic aqueous solution with a

* Corresponding author. E-mail: zhaobaoxiu@tsinghua.org.cn

semiconductor photocatalytic reaction. Besides the photocatalytic oxidation degradation for POPs, semiconductor photocatalysis also has the ability to reduce organic compounds. Actually photocatalytic reduction is an alternative pathway for the degradation of poly- or per-halogenated organic compounds which are difficult to oxidize further. For example, the simplest perchloroalkane, i.e., CCl_4 was photo-reductively degraded by TiO_2 in the presence of organic electron donors (Chio and Hoffmann, 1995), and ZnS and CdS were also used as photocatalysts for the reductive dehalogenation of halogenated benzene derivatives (Yin et al., 2001).

Ga_2O_3 is a wide bandgap semiconductor and it is mainly used in the photoelectronic field (Zheng et al., 2007); nevertheless it is rarely used as a photocatalyst in wastewater treatment. Compared with TiO_2 (E_g = 3.2 eV, E_{cb} = 4.21 eV), Ga_2O_3 possesses a wider bandgap (E_g = 4.8 eV) and higher conduction band position (E_{cb} = –2.95 eV). Thus, theoretically, the reduction potential of Ga_2O_3 is higher than that of TiO_2, which implies that it is possible for Ga_2O_3 to decompose PFOA. Based on this, we first investigated the photocatalytic decomposition of PFOA with β-Ga_2O_3 in anoxic solution and then deduced the decomposition mechanism.

1 Materials and methods

1.1 Materials

PFCAs (purity > 98%), including PFOA ($C_7F_{15}COOH$), perfluoroheptanoic acid ($C_6F_{13}COOH$), perfluorohexanoic acid ($C_5F_{11}COOH$), perfluoropentanoic acid (C_4F_9COOH), perfluorobutyric acid (C_3F_7COOH), perfluoropropionic acid (C_2F_5COOH) and trifluoroformyl acid (TFA, CF_3COOH), were all purchased from Aldrich Co. (USA). α-Ga_2O_3 powder (purity ⩾ 99.9%) was purchased from Aladdin Reagent Co. (China). Methanol, thiosulfate and oxalate were all analytical reagents and purchased from Chemical Reagent Co. (China). High purity water (18.2 MΩ/cm) used in all experiments was prepared using the Thermo Scientific Barnstead Nanopure Diamond UV^{TM} water purification system (Thermo Scientific, USA).

1.2 Preparation of β-Ga_2O_3 and characterizations

Using α-Ga_2O_3 as raw material, β-Ga_2O_3 was successfully prepared through calcination at 800°C for 4 hr in air. The crystalline phase of β-Ga_2O_3 was analyzed by an X-ray diffraction (XRD) instrument monitored by a D/max-RB system (Cu $K_{\alpha 1}$ irradiation, λ = 1.5406 Å, voltage = 40 kV, current = 30 mA, scanning rate = 0.01°/sec, scanning range = 10°–80°). Based on the Brunauer-Emmett-Teller (BET) equation, Ga_2O_3 specific surface areas were obtained using the nitrogen sorption-desorption equipment (NOVA4000, Germany) at 77.3 K. The bandgap energy was derived from the UV-Vis diffuse reflection spectrum measured with a UV-Vis NIR spectrometer (Varian Cary 500, USA).

1.3 Photocatalytic degradation procedure

Photocatalytic degradation of PFOA was performed in a cylindrical quartz reactor with a glass jacket for cooling water circulation. PFOA aqueous solution (100 mL, 75 μmol/L) containing 0.5 g/L β-Ga_2O_3 powder was transferred to the reactor. The UV-C light (λ = 254 nm) was irradiated using a 15 W low-pressure mercury lamp which was placed in the center of the reactor, equipped with a protective quartz tube. High-purity nitrogen gas (P > 99.99%) was supplied to the solution with a flow rate of 40 mL/min. The mixed solution containing PFOA and β-Ga_2O_3 was first bubbled for 3 hr to ensure that the adsorption of PFOA on β-Ga_2O_3 surface and reactor interior had reached equilibrium (in this experiment, the adsorption for PFOA was about 6.4% after 3 hr accompanied with bubbling N_2), then the reaction was started. The initial pH of the PFOA solution (75 μmol/L) was about 4.8 and was not adjusted in the following experiments.

1.4 Ion chromatography

The concentrations of F^-, $S_2O_3^{2-}$ and SO_4^{2-} were measured with an Ion Chromatography System (ICS-2000, Dionex, Sunnyvale, USA) equipped with an automatic elution generator and separation column (Dionex Ionpac AS11). The column temperature was maintained at 30°C and the injection volume was kept at 25 μL. The eluting phase containing 30 mmol/L KOH was automatically produced by the electrolysis apparatus connected with the chromatography system and the flow rate was set at 1.2 mL/min. Before analysis, all samples were filtered with a 0.45 μm PFTE membrane to remove β-Ga_2O_3 particles.

1.5 LC-MS and LC-MS/MS analysis

The concentrations of PFOA and shorter-chain PFCAs were measured by a Waters Acquity Ultra Performance Liquid Chromatography (LC) system linked with a micromass Quattro Premier Tandem Quadrupole mass spectrometer (Waters, USA). The electrospray negative ion (ESI^-) mode was adopted. The mobile phase consisted of 2 mmol/L ammonium acetate (named as solvent A) and 2 mmol/L ammonium acetate/methanol (named as solvent B), and the flow rate was 0.4 mL/min. A gradient flow mode was used and the flow sequences were as follows: 0–0.5 min, isocratic flow of 30% solvent B and 70% solvent A; 0.5–5.0 min, linear increase of solvent B from 30% to 90%; 5.0–5.1 min: linear increase of solvent B from 90% to 100%; 5.1–6.0 min: hold solvent B at 100%; 6.0–7.0 min: linear decrease of solvent B from 100% to 30%; 7.0–10.0 min: hold solvent B at 30%. Samples were managed by an auto-sampler (Waters, USA) and separated by an Acquity BEH C_{18} column (2.1 mm × 50 mm, 1.7 μm). Data acquisition of chromatograms or mass spectra was controlled by the MassLynx V 4.1 software. The MS full scan spectrum ranged from m/z 100 to 420 and the scan time was 10.0 min. The concentrations of PFOA and shorter-chain PFCAs were measured with a 7-channel MRM mode. Here, all samples were diluted below 1.0 mg/L and filtered by a 0.22 μm PFTE ultra-filtration

membrane before analysis.

2 Results and discussion

2.1 Characterizations of β-Ga_2O_3

The Ga_2O_3 crystal phase can be characterized by XRD patterns. Figure 1 displays the crystallization of commercial α-Ga_2O_3 and as-prepared β-Ga_2O_3. Several characteristic diffraction peaks which belong to the β phase (JCPDS No: 43-1012) clearly appear in the XRD pattern, which shows that β-Ga_2O_3 can be obtained by the dry calcination method using α-Ga_2O_3 as raw material. According to the BET equation, the specific surface area of as-prepared β-Ga_2O_3 decreases slightly to 27.8 m^2/g, compared with that of α-Ga_2O_3 (32.1 m^2/g), which suggests that a few particles co-aggregate during the transformation of the crystal phase.

The bandgap energy (E_g) of as-prepared β-Ga_2O_3 can be obtained from the UV-Vis diffuse reflection spectrum (Fig. 2). The value of E_g (4.7 eV) can be obtained from the intersection point (258 nm) of the tangent and the *X*-axis, which is in agreement with the reported value of 4.8 eV for pure powder (Xu and Schoonen, 2005).

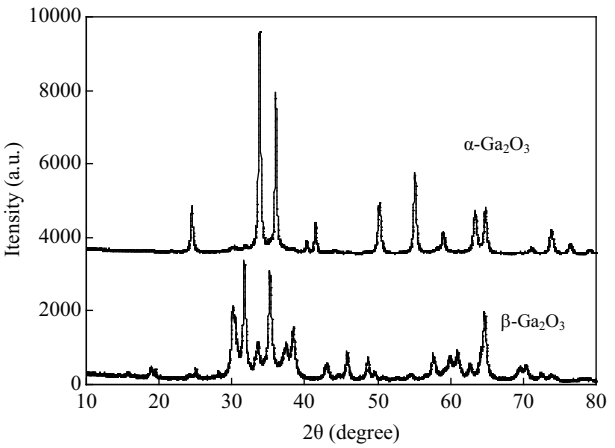

Fig. 1 X-ray diffraction patterns of α-Ga_2O_3 and β-Ga_2O_3 prepared by calcination at 800°C for 4 hr in air.

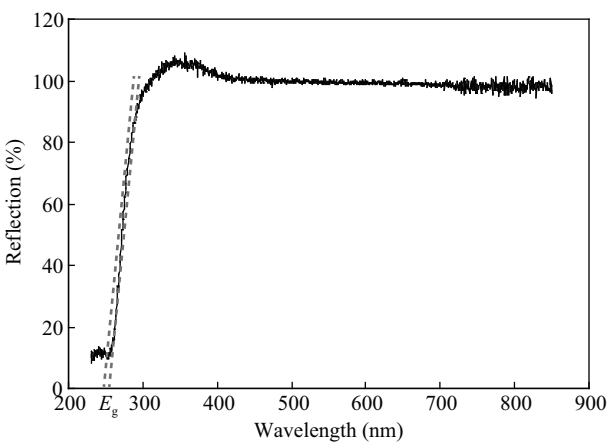

Fig. 2 UV-Vis diffuse reflection spectrum of as-prepared β-Ga_2O_3.

2.2 Photocatalytic decomposition

Three experiments including direct photodegradation and β-Ga_2O_3 photocatalytic degradation in the presence of N_2 or O_2 were carried out. From Fig. 3, it appears that PFOA is hardly destroyed by direct photodegradation, only 4.8% PFOA is degraded after 3 hr, and 43.6% PFOA is destroyed in the presence of N_2, but only 10.7% PFOA is decomposed when O_2 instead of N_2 is supplied. This is to say that the photoinduced hole or HO· is not the protagonist decomposing PFOA. Thus the sole actor involved in PFOA degradation is photoinduced electrons (e^-_{cb}). In fact, e^-_{cb} has a powerful ability to reduce halogen-containing compounds through dehalogenation reactions (Chio and Hoffmann, 1995). The conclusion that PFOA is destroyed by e^-_{cb} can be explained by the bandgap structures of β-Ga_2O_3 and TiO_2. β-Ga_2O_3 has a more negative reduction potential (–1.55 V (NHE)) than TiO_2 (–0.29 V (NHE)). This reveals that e^-_{cb} coming from the β-Ga_2O_3 possesses a more powerful reduction ability, compared with that coming from TiO_2.

2.3 Photocatalytic defluorination

To research the fate of fluorine atoms, the F^- concentration was measured. Here, defluorination (*R*, %) and transformation degree of fluorine (denoted as D_F) are introduced and defined by Eqs. (1) and (2).

$$R(\%) = \frac{C_{F^-} \times 100}{15 \times C_{PFOA_0}} \quad (1)$$

$$D_F = \frac{C_{F^-}}{15 \times (C_{PFOA_0} - C_{PFOA_t})} \quad (2)$$

where, C_{F^-} is the molar concentration of fluoride ions; C_{PFOA_0} and C_{PFOA_t} are the initial and *t* time molar concentrations of PFOA, respectively. The relationship of defluorination and D_F with reaction time is shown in Fig. 4. It is observed that defluorination increases with reaction time and arrives at 15.7% after 3 hr, while D_F changes only a little from 0.273 at 30 min to 0.286 at 3 hr, which suggests that the relationship between the generation of F^- and degradation of PFOA is fixed. This is to say that about four fluorine atoms are transformed to F^- and released

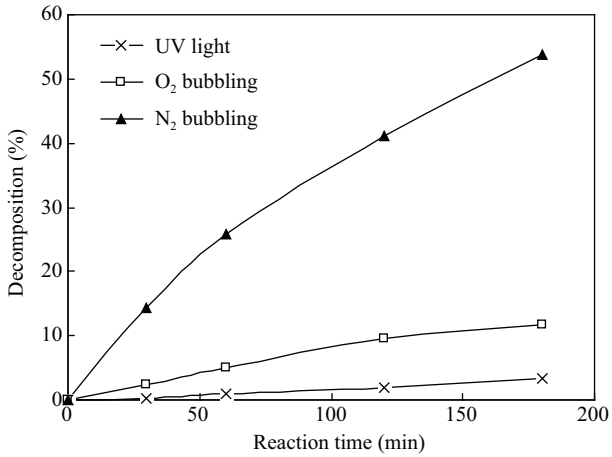

Fig. 3 (a) Direct photodegradation and β-Ga_2O_3 photocatalytic decomposition in the presence of N_2 or O_2, respectively.

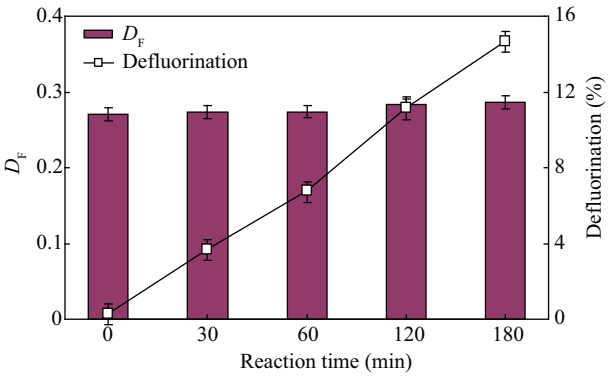

Fig. 4 The relationship of D_F and defluorination with reaction time in the β-Ga_2O_3 photocatalytic degradation reaction. Where, $[PFOA]_0$: 75 μmol/L; power of UV light: 15 W; dosage of β-Ga_2O_3: 0.5 g/L; flow rate of N_2: 40 mL/min; without pH adjustment.

to the solution when one molecule PFOA is completely degraded, and the remaining fluorine atoms may exist in other intermediates.

2.4 Effect of pH on photocatalytic decomposition

pH is one of the important factors in the photocatalytic reaction, because it influences the charge state of the photocatalyst and ionization degree of the pollutant. The photocatalytic decomposition of PFOA was conducted at four different pH values, i.e., 4, 7, 9, and 11, and results are presented in Fig. 5. The results show that the decomposition efficiency decreases with increasing pH. Although the most-cited pK_a value of PFOA is 2.8 in the literature (Goss, 2008), recently an argument has been put forth that the pK_a value of PFOA may be as low as –0.5 based on analogy considerations and molecular modeling. According to this estimated pK_a value, PFOA molecules completely ionize in the investigated pH range (pH 4–11) and exist in the form of $C_7F_{15}COO^-$ anions. The above analysis can be approved by the following Reaction (3) and Eqs. (4) and (5).

$$C_7F_{15}COOH \longrightarrow C_7F_{15}COO^- + H^+ \quad (3)$$

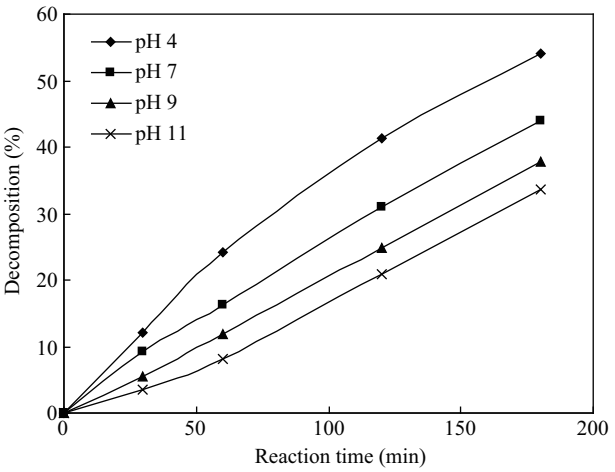

Fig. 5 The effect of pH on β-Ga_2O_3 photocatalytic degradation of PFOA in the presence of bubbling N_2. The pH of the aqueous solution was adjusted with H_2SO_4 or NaOH. $[PFOA]_0$: 75 μmol/L; power of UV light: 15 W; dosage of β-Ga_2O_3: 0.5 g/L; flow rate of N_2: 40 mL/min.

$$K_a = \frac{C_{H^+} \times C_{C_7F_{15}COO^-}}{C_{C_7F_{15}COOH}} = \frac{10^{-pH} \times C_{C_7F_{15}COO^-}}{C_0 - C_{C_7F_{15}COO^-}} \quad (4)$$

$$C_{C_7F_{15}COO^-} = \frac{K_a \times C_0}{10^{-pH} + K_a} \approx C_0 \quad (5)$$

where, C_0 is the initial concentration of PFOA. According to Eq. (3), it is observed that the change of pH (4–11) does not affect the ionization of PFOA. However, pH change definitely influences the surface charge state of β-Ga_2O_3. The reported isoelectric point (IEP) of β-Ga_2O_3 is about pH 9 (Kosmulski, 2001), so the surface charge of β-Ga_2O_3 becomes positive when the pH is lower than 9, which is beneficial for the adsorption for $C_7F_{15}COO^-$ anions on the β-Ga_2O_3 surface, and negative when the pH is higher than 9, which repels the adsorption of $C_7F_{15}COO^-$ anions on the β-Ga_2O_3 surface. As is well known, photocatalytic reaction mainly occurs on the surface of the catalyst, so it is reasonable that the photocatalytic decomposition for PFOA performs better in lower pH solutions where $C_7F_{15}COO$ is more easily adsorbed on the surface of β-Ga_2O_3.

2.5 Effect of reductive additives on photocatalytic degradation

Based on the above analysis, it is observed that PFOA is decomposed well under a reductive atmosphere. Although N_2 bubbling can drive dissolved O_2 out of an aqueous solution to an utmost degree, residual dissolved O_2 still reacts with e^-_{cb} to produce H_2O_2, weakening the concentration of e^-_{cb}.

To further drive dissolved O_2 and H_2O_2 out of the reaction system, methanol (CH_3OH), $S_2O_3^{2-}$ and oxalate ($C_2O_4^{2-}$) reductive reagents were studied and results are shown in Table 1. Before the investigation on the effects of reductive additives on PFOA degradation, corresponding blank experiments were carried out and results showed that the influences of reductive additives were slight (removal efficiency < 4.6%). It is clearly observed that the addition of reductive reagents accelerates the degradation and defluorination of PFOA, and $S_2O_3^{2-}$ performs best. To some extent, degradation increases with increasing amount of $S_2O_3^{2-}$, and the reason can be explained by the following Reactions ((6)–(7)).

$$2S_2O_3^{2-} + 3O_2 \longrightarrow 2SO_4^{2-} + 2SO_2 \quad (6)$$

$$S_2O_3^{2-} + 4H_2O_2 \longrightarrow 2SO_4^{2-} + 3H_2O + 2H^+ \quad (7)$$

Furthermore, a phenomenon is observed that the concentration of $S_2O_3^{2-}$ decreases with the reaction time and almost all $S_2O_3^{2-}$ is transformed to SO_4^{2-} at last, suggesting that $S_2O_3^{2-}$ is indeed oxidized by O_2 or H_2O_2.

2.6 Major intermediates and degradation mechanism

As mentioned above, F^- is one of the major intermediates in aqueous solution. To further analyze other major products in the liquid phase, a LC-MS full scan was carried out and the spectrum is presented in Fig. 6. Compared with the inset MS full scan spectrum of the PFOA standard

Table 1 Photocatalytic decomposition and defluorination of PFOA with β-Ga_2O_3 in the presence of reductive reagent and bubbling N_2

Additives	No additive	CH_3OH 50 (μmol/L)	$C_2O_4^{2-}$ 50 (μmol/L)	$S_2O_3^{2-}$ 20 (μmol/L)	$S_2O_3^{2-}$ 50 (μmol/L)	$S_2O_3^{2-}$ 75 (μmol/L)
Decomposition (%)	43.6	85.4	82.3	72.6	98.8	96.1
Defluorination (%)	14.7	25.6	23.4	21.3	31.6	28.8
Rate constant (min^{-1})	0.0042	0.0186	0.0169	0.0127	0.0239	0.0214
Half time (hr)	2.7	0.62	0.68	0.91	0.48	0.54

$[PFOA]_0$ was 75 μmol/L; pH of PFOA aqueous solution was not adjusted. The dosage of β-Ga_2O_3 was 0.5 g/L. Flow rate of N_2 was 40 mL/min.

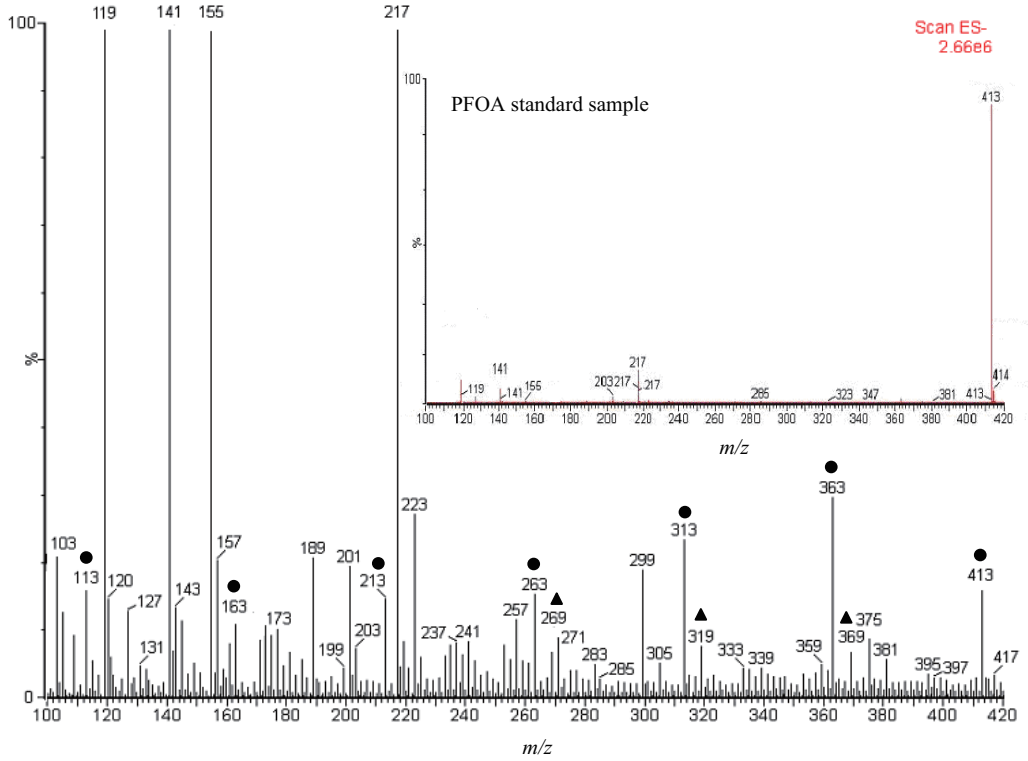

Fig. 6 MS full scan spectrum of PFOA aqueous solution sample photocatalytically decomposed by β-Ga_2O_3 for 3 hr in the presence of $S_2O_3^{2-}$ and bubbling N_2, and the inset is the MS spectrum of the PFOA standard sample.

sample, one series of obvious peaks appears at *m/z* 413, 363, 313, 263, 213, 163, 113 and the *m/z* differences between the neighboring peaks are 50. They are assigned to $[C_nF_{2n+1}COO]^-$ ($1 \leqslant n \leqslant 7$) and the *m/z* difference is caused by the loss of the $-CF_2$ group, which reveals that shorter-chain PFCAs are major intermediates in the reduction reaction. Another series of peaks is present at *m/z* 369, 319, and 269 and the *m/z* differences between the neighboring peaks are also 50. These peaks are assigned to $[C_nF_{2n+1}]^-$ ($5 \leqslant n \leqslant 7$) groups which originate from $C_nF_{2n+1}H$ ($5 \leqslant n \leqslant 7$). Because $C_nF_{2n+1}H$ ($2 \leqslant n \leqslant 4$) molecules are gaseous under normal conditions and easily escape from the solution, the peaks at *m/z* 219, 169 and 119 are not observed in the MS spectrum. Besides these characteristic peaks, there appear intense peaks at *m/z* 119, 141, 155, 217, but they also emerge in the spectrum of the PFOA standard sample. These peaks are probably caused by solvents or impurities from the PFOA sample.

In the photochemical and sonochemical degradation reactions, the decomposition mechanism involves three steps: decarboxylation of PFOA, elimination of HF from $C_7F_{15}OH$ and hydrolysis of $C_6F_{13}COF$. Based on the MS spectrum and chromatograms, the β-Ga_2O_3 photocatalytic decomposition mechanism can be deduced. First, PFOA is ionized to $C_7F_{15}COO^-$ and H^+ in water:

Then the $C_7F_{15}COO^-$ absorbs on the surface of β-Ga_2O_3 and reacts with $e^-_{cb,}$ forming C_7F_{15}•:

$$C_7F_{15}COO^- \xrightarrow{e^-_{cb}} C_7F_{15}COO\bullet^{2-} \xrightarrow{H^+} HO^- + C_7F_{15}CO\bullet \longrightarrow C_7F_{15}\bullet + CO \quad (8)$$

There is a similar study showing that PFOA can be reductively degraded into C_7F_{15}· and CO by a hydrated electron (e^-_{aq}) (Park et al., 2009). The C_7F_{15}· produced is very active and quickly reacts with H_2O to form $C_7F_{15}OH$. $C_7F_{15}OH$ is unstable and easily loses HF, generating $C_6F_{13}COF$ which easily hydrolyzes to form $C_6H_{13}COOH$. Then, step by step, $C_5H_{11}COOH$, C_4H_9COOH, C_3H_7COOH, C_2H_5COOH and CH_3COOH are produced. In fact, Yamamoto et al. (2007) also observed shorter-chain PFCAs during photodegradation of PFOS in the presence of alkaline 2-propanol and bubbling N_2. Perhaps due to a low photodegradation decomposition efficiency (k = 0.93 day^{-1}), only $C_7F_{15}COOH$, $C_6F_{13}COOH$, $C_5F_{11}COOH$ were measured. That is to say that shorter-chain PFCAs

are major organic products during PFOA degradation with the reduction method.

3 Conclusions

PFOA was efficiently decomposed by β-Ga_2O_3 photocatalytic reduction and photoinduced electrons were the effective species destroying PFOA in anoxic aqueous solution. Photocatalytic degradation and defluorination of PFOA was 98.8% and 31.6% in the presence of $S_2O_3^{2-}$ and bubbling N_2, respectively. Photocatalytic decomposition followed first-order kinetics (k = 0.0239 min^{-1}, $t_{1/2}$ = 0.48 hr), and F^- and shorter-chain PFCAs were the major products during PFOA degradation. Reductive decarboxylation of PFOA was the crucial pathway in the β-Ga_2O_3photocatalytic reaction.

Acknowledgments

This work was supported by the National Natural Science Foundation of China (No. 20907026) and the High Level Talent Research Foundation of Qindao Technological University (No: C-10-210). The authors would like to thank Dr. Colin Zhao for English revision in grammar and structures.

References

Bischel H N, MacManus-Spencer L A, Luthy R G, 2010. Noncovalent interactions of long-chain perfluoroalkyl acids with serum albumin. *Environmental Science and Technology*, 44(13): 5263–5269.

Cheng J, Vecitis C D, Park H, Mader B T, Hoffman M R, 2008. Sonochemical degradation of perfluorooctane sulfonate (PFOS) and perfluorooctanoate (PFOA) in landfill groundwater: environmental matrix effects. *Environmental Science and Technology*, 42(21): 8057–8063.

Cheng J, Vecitis C D, Park H, Mader B T, Hoffman M R, 2010. Sonochemical degradation of perfluorooctane sulfonate (PFOS) and perfluorooctanoate (PFOA) in groundwater: kinetic effects of matrix inorganics. *Environmental Science and Technology*, 41(1): 445–450.

Choi W Y, Hoffmann M R, 1995. Photoreductive mechanism of CCl_4 degradation on TiO_2 particles and effects of electron donors. *Environmental Science and Technology*, 29(6): 1646–1654.

Dillert R, Bahnemann D, Hidaka H, 2007. Light-induced degradation of perfluorocarboxylic acids in the presence of titanium dioxide. *Chemosphere*, 67(4): 785–792.

Goss K U, 2008. The pK_a values of PFOA and other highly fluorinated carboxylic acids. *Environmental Science and Technology*, 42(2): 456–458.

Hansen K J, Johnson H O, Eldridge J S, Butenhoff J L, Dick L A, 2002. Quantitative characterization of trace levels of PFOS and PFOA in the Tennessee River. *Environmental Science and Technology*, 36(8): 1861–1865.

Hori H, Hayakawa E, Einaga H, Kutsuna S, Koike K, Ibusuki T et al., 2004. Decomposition of environmentally persistent perfluorooctanoic acid in water by photochemical approaches. *Environmental Science and Technology*, 38(22): 6118–6124.

Hori H, Nagoka Y, Murayama M, Kutsuna S, 2008. Efficient decomposition of perfluorocarboxylic acids and alternative fluorochemical surfactants in hot water. *Environmental Science and Technology*, 42(19): 7438–7443.

Hori H, Yamamoto A, Hayakawa E, Taniyasu S, Yamashita N, Kutsuna S et al., 2005. Efficient decomposition of environmentally persistent perfluorocarboxylic acids by use of persulfate as a photochemical oxidant. *Environmental Science and Technology*, 39(7): 2383–2388.

Houde M, Martin W J, Letcher J R, Solomon K R, Muir D C G, 2006. Biological monitoring of polyfluoroalkyl substances: a review. *Environmental Science and Technology*, 40(11): 3463–3473.

Kannan K, Perrotta E, Thomas N J, 2006. Association between perfluorinated compounds and pathological conditions in southern sea otters. *Environmental Science and Technology*, 40(16): 4943–4948.

Kosmulski M, 2001. Pristine points of zero charge of gallium and indium oxides. *Journal of Colloid Interface Science*, 238(1): 225–227.

Kudo N, Suzuki E, Katakura M, Ohmori K, Noshiro R, Kawashima Y, 2001. Comparison of the elimination between perfluorinated fatty acids with different carbon chain length in rats. *Chemico-Biological Interactions* 134(2): 203–216.

Martin J W, Smithwick M M, Braune B M, Hoekstra P F, Muir D D G, Mabury S A, 2004. Identification of long-chain perfluorinated acids in biota from the Canadian Arctic. *Environmental Science and Technology* 38(2): 373–380.

Moriwaki H, Takagi Y, Tanaka M, Tsuruho K, Okitsu K, Maeda Y, 2005. Sonochemical decomposition of perfluorooctane sulfonate and perfluorooctanoic acid. *Environmental Science and Technology*, 39(9): 3388–3392.

Niisoe T, Harada K H, Ishikawa H, Koizumi A, 2010. Long-term simulation of human exposure to atmospheric perfluorooctanoic acid (PFOA) and perfluorooctanoate (PFO) in the Osaka urban area, Japan. *Environmental Science and Technology*, 44(20): 7852–7857.

Panchangam S C, Lin A Y C, Shaik K L, Lin C F, 2009. Decomposition of perfluorocarboxylic acids (PFCAs) by heterogeneous photocatalysis in acidic aqueous medium. *Chemosphere*, 77(2): 242–248.

Park H, Vecitis C D, Cheng J, Choi W, Mader B T, Hoffman M R, 2009. Reductive defluorination of aqueous perfluorinated alkyl surfactants: effects of ionic headgroup and chain length. *The Journal of Physical Chemistry A*, 113(4): 690–696.

Pistocchi A, Loos R, 2009. A map of European emissions and concentrations of PFOS and PFOA. *Environmental Science and Technology*, 43(24): 9237–9244.

Scott B A, Spencer C S, Mabury A D, Muir D D G, 2006. Poly and perfluorinated carboxylates in North American precipitation *Environmental Science and Technology* 40(23): 7167–7174.

So M K, Taniyasu S, Yamashita N, Giesy J P, Zheng J, Fang Z et al., 2004. Perfluorinated compounds in coastal waters of Hong Kong, South China, and Korea. *Environmental Science and Technology*, 38(15): 4056–4063.

Tao L, Ma J, Kunisue T, Libelo E L, Tanabe S, Kannan K, 2008. Perfluorinated compounds in human breast milk from several Asian countries, and in infant formula and dairy milk from the United States. *Environmental Science and Technology*, 42(22): 8597–8602.

Vecitis C D, Park H, Cheng J, Mader B T, Hoffmann M R, 2008. Kinetics and mechanism of the sonolytic conversion of

the aqueous perfluorinated surfactants, perfluorooctanoate (PFOA), and perfluorooctane sulfonate (PFOS) into inorganic products. *The Journal of Physical Chemistry A*, 112(18): 4261–4270.

Xu Y, Schoonen M A A, 2005. The absolute energy positions of conduction and valence bands of selected semiconducting minerals. *American Mineralogist*, 85(3-4): 543–556.

Yamamoto T, Noma Y, Sakai S I, Shibata Y, 2007. Photodegradation of perfluorooctane sulfonate by UV irradiation in water and alkaline 2-propanol. *Environmental Science and Technology*, 41(16): 5660–5665.

Yin H B, Wada Y, Kitamura T, Yanagida S, 2001. Photoreductive dehalogenation of halogenated benzene derivatives using ZnS or CdS nanocrystallites as photocatalysts. *Environmental Science and Technology*, 35(1): 227–231.

Zheng J F, Tsai W, Lin T D, Lee Y J, Chen C P, Hong M et al., 2007. Ga_2O_3 (Gd_2O_3)/Si_3N_4 dual-layer gate dielectric for InGaAs enhancement mode metal-oxide-semiconductor field-effect transistor with channel inversion *Applied Physics Letters*, 91(22): 223502.

JOURNAL OF ENVIRONMENTAL SCIENCES

Journal of Environmental Sciences (Established in 1989)
Vol. 24 No. 4 2012

Supervised by	Chinese Academy of Sciences	**Published by**	Science Press, Beijing, China
Sponsored by	Research Center for Eco-Environmental		Elsevier Limited, The Netherlands
	Sciences, Chinese Academy of Sciences	**Distributed by**	
Edited by	Editorial Office of Journal of	Domestic	Science Press, 16 Donghuangchenggen
	Environmental Sciences (JES)		North Street, Beijing 100717, China
	P. O. Box 2871, Beijing 100085, China		Local Post Offices through China
	Tel: 86-10-62920553; http://www.jesc.ac.cn	Foreign	Elsevier Limited
	E-mail: jesc@263.net, jesc@rcees.ac.cn		http://www.elsevier.com/locate/jes
Editor-in-chief	Hongxiao Tang	**Printed by**	Beijing Beilin Printing House, 100083, China

CN 11-2629/X **Domestic postcode: 2-580** **Domestic price per issue RMB ¥ 110.00**

ISSN 1001-0742